

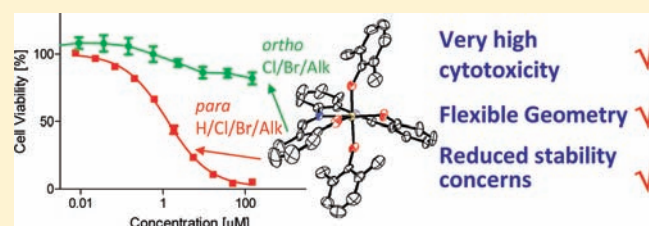
Cytotoxicity and Hydrolysis of *trans*-Ti(IV) Complexes of Salen Ligands: Structure–Activity Relationship Studies

Avia Tzuberly and Edit Y. Tshuva*

Institute of Chemistry, The Hebrew University of Jerusalem, 91904, Jerusalem, Israel

Supporting Information

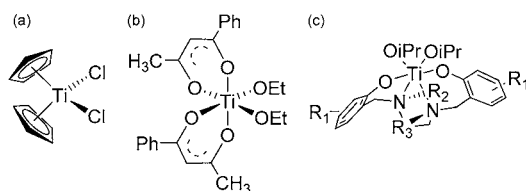
ABSTRACT: Eleven bis(dimethylphenolato) Ti(IV) complexes of salen ligands with different steric and electronic properties due to different aromatic substituents at the ortho and para positions are reported, and their cytotoxicity toward HT-29 and OVCAR-1 cells and its dependence on hydrolytic behavior are discussed. Eight complexes of this series were analyzed by X-ray crystallography, confirming the trans geometry of the labile ligands with otherwise relatively similar coordination features to those of *cis*-salen analogues. Relatively high and similar hydrolytic stability is observed for all complexes, with $t_{1/2}$ values for labile ligand hydrolysis of 2–11 h in 10% D₂O solutions. In contrast, varying cytotoxicities were achieved, identifying selected members as the first *trans*-Ti(IV) complexes reported as anticancer agents. Steric bulk all around the complex diminished the activity, where a complex with no aromatic substitutions is especially active and complexes substituted particularly at the ortho positions are mostly inactive, including *ortho*-halogenated and *ortho-tert*-butylated, with one exception of the *ortho*-methoxylated complex demonstrating appreciable activity. In contrast, *para*-halogenation provided the complexes of highest cytotoxic activity in this series (IC₅₀ as low as 1.0 ± 0.3 μM), with activity exceeding that of cisplatin by up to 15-fold. Reaction of a representative complex with *ortho*-catechol yielded a “*cis*”-Ti(IV) complex following rearrangement of the salen ligand on the metal center, with highly similar coordination features and geometry to those of the catecholato salen analogues, suggesting that the complexes operate by similar mechanisms and rearrangement of the salen ligand may occur upon introduction of a suitable chelating target. In additional cytotoxicity measurements, a salen complex was preincubated in the biological medium for varying periods prior to cell addition, revealing that marked cytotoxicity of the salen complex is retained for longer preincubation periods relative to known Ti(IV) complexes, suggesting that the hydrolysis products may also induce cytotoxic effects, thus reducing stability concerns.



INTRODUCTION

Cisplatin, the first inorganic compound approved as an anticancer agent, is widely used worldwide along with its derivatives.^{1–5} Nevertheless, its disadvantages relating to high toxicity and limited activity range encourage extensive research aimed at finding new inorganic complexes of other metal centers that may lead to different and improved anticancer drugs.^{6–15} Among others, titanium(IV) complexes have shown high antitumor activity, where in particular titanocene dichloride (Cp₂TiCl₂, Scheme 1, a) and budotitane ((bzac)₂Ti(OEt)₂,

Scheme 1. Titanocene Dichloride (a), Budotitane (b), and Salen Complexes (c)



Scheme 1, b), followed by their improved derivatives with different substitutions, demonstrated promising activity toward

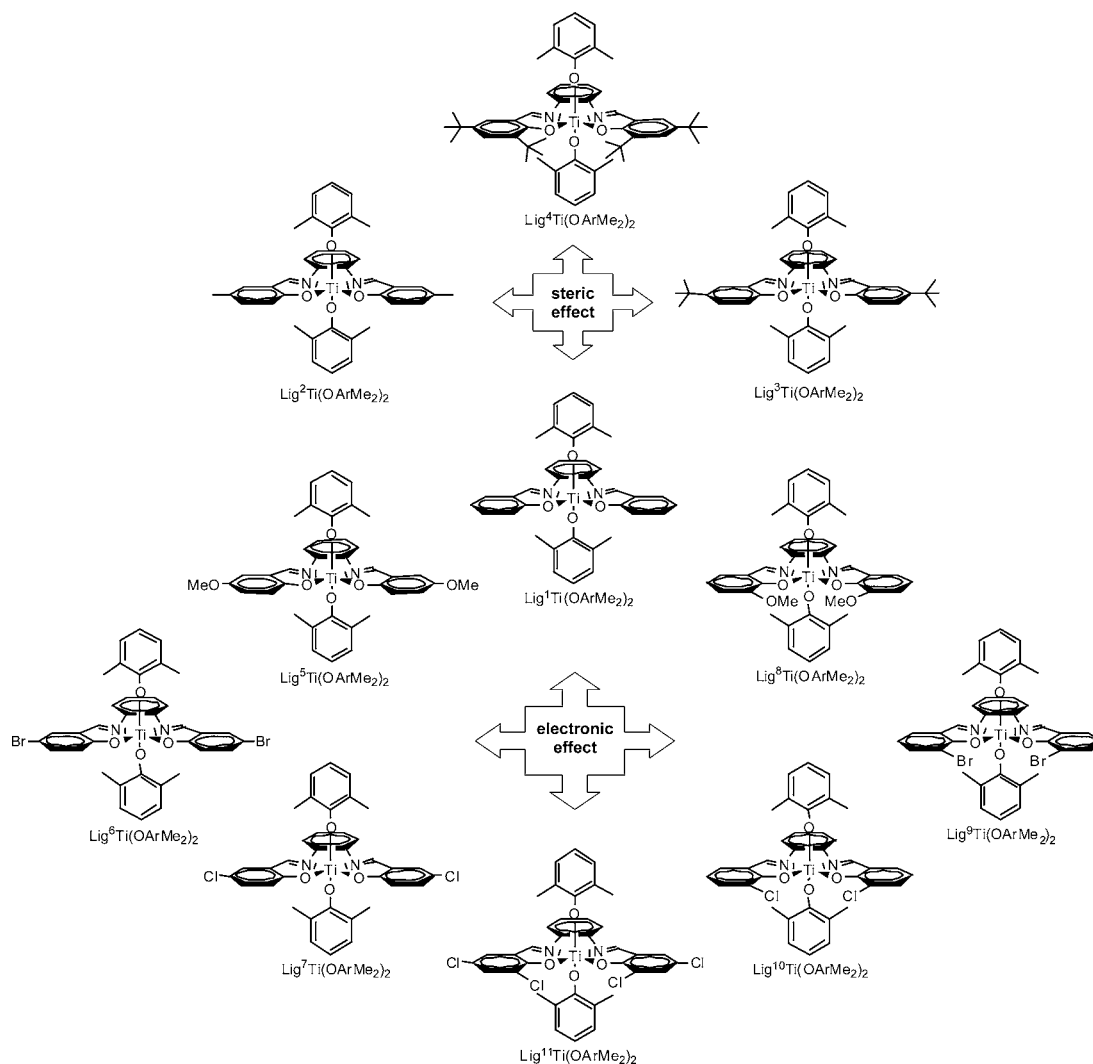
cisplatin-sensitive and -resistant cells with relatively minor toxicity.^{16–25} The main disadvantage of the Ti(IV) complexes is, however, their relatively rapid hydrolysis in biological environment,^{19,21,26,27} where the labile ligands of Cp₂TiCl₂ and (bzac)₂Ti(OEt)₂ (Cl, OEt) dissociate within seconds to minutes while the inert ligands (Cp, diketonato) hydrolyze within hours to give undefined aggregates, thus hampering mechanistic investigations and applicability.

We previously introduced the family of cytotoxic Ti(IV) complexes based on diamino bis(phenolato), salen ligands (Scheme 1c).^{28–32} Complexes of this family have demonstrated high cytotoxic activity along with exceptional hydrolytic stability. Structure–activity relationship studies have revealed that the ligand and its particular substitutions play an important role in determining the complex performance, where the hydrolytic behavior of the complexes and their cytotoxicity are closely related.^{28,29} All such titanium(IV) complexes investigated thus far as cytotoxic agents feature two labile ligands in a *cis* configuration and were designed as such under the assumption that dissociation of the labile ligands enables

Received: September 26, 2011

Published: December 29, 2011

Chart 1. Salen Complexes Investigated



potential chelate binding to a biological target, as occurs for cisplatin.^{1–4} In particular, transplatin lacks meaningful activity due to the inability to form a 1,2-intrastrand cross-link to two adjacent bases in DNA, although other *trans*-platinum complexes exhibit cytotoxic properties by different mechanisms.³³ As the mechanism of cytotoxic activity of the titanium(IV) complexes and their binding form to the cellular target remain unknown, the requirement of this structural feature is yet undetermined. In our recent communication³⁴ we reported on the first family of highly cytotoxic *trans*-Ti(IV) complexes based on salen ligands, which include similar donor atoms to those of the salen ligands, only known to prefer equatorial binding due to the planar imine moiety leading to *trans*-labile ligands (Chart 1).^{35,36} We employed the salophen ligands that include a planar phenylenediamine bridge,^{37–39} found to more conveniently yield pure products. Herein we elaborate on this family of complexes, with detailed structure–activity relationship investigations that reveal the parameters of influence on the cytotoxic activity of these complexes toward colon HT-29 and ovarian OVCAR-1 cells and their hydrolytic stability while shedding light on their possible binding mechanism.

RESULTS AND DISCUSSION

Synthesis and Characterization. Ligands $\text{H}_2\text{Lig}^{1–11}$ were prepared according to known procedures via a single step of a condensation reaction between the substituted salicylaldehyde compounds and phenylenediamine.^{40,41} The ligand structure was determined mainly by ^1H and ^{13}C NMR. The complexes $\text{Lig}^{1–11}\text{-Ti}(\text{OArMe}_2)_2$ were prepared in analogy to known compounds by stirring the ligands $\text{H}_2\text{Lig}^{1–11}$ with 1 equiv of $\text{Ti}(\text{OArMe}_2)_4$, prepared as previously described from $\text{Ti}(\text{OiPr})_4$,⁴² at room temperature in THF under an inert atmosphere to give the Ti(IV) complexes in high yields.³⁴ The precursor $\text{Ti}(\text{OArMe}_2)_4$ was selected due to difficulties in isolating pure complexes when starting from $\text{Ti}(\text{OiPr})_4$ and previous reports on lesser influence of the labile ligands on cytotoxicity.²¹ The complexes were analyzed by NMR, featuring a single set of signals for the phenolato moiety of the salen ligand and a single type of a labile ligand.

Further support for the complexes structures came from X-ray crystallography. $\text{Lig}^{1–4,7–10}\text{-Ti}(\text{OArMe}_2)_2$ were crystallized to produce red single crystals that were crystallographically analyzed.³⁴ $\text{Lig}^4\text{-Ti}(\text{OArMe}_2)_2$ was crystallized from hexane, while the rest were crystallized from diethyl ether. The ORTEP drawings of these complexes along with lists of selected bond

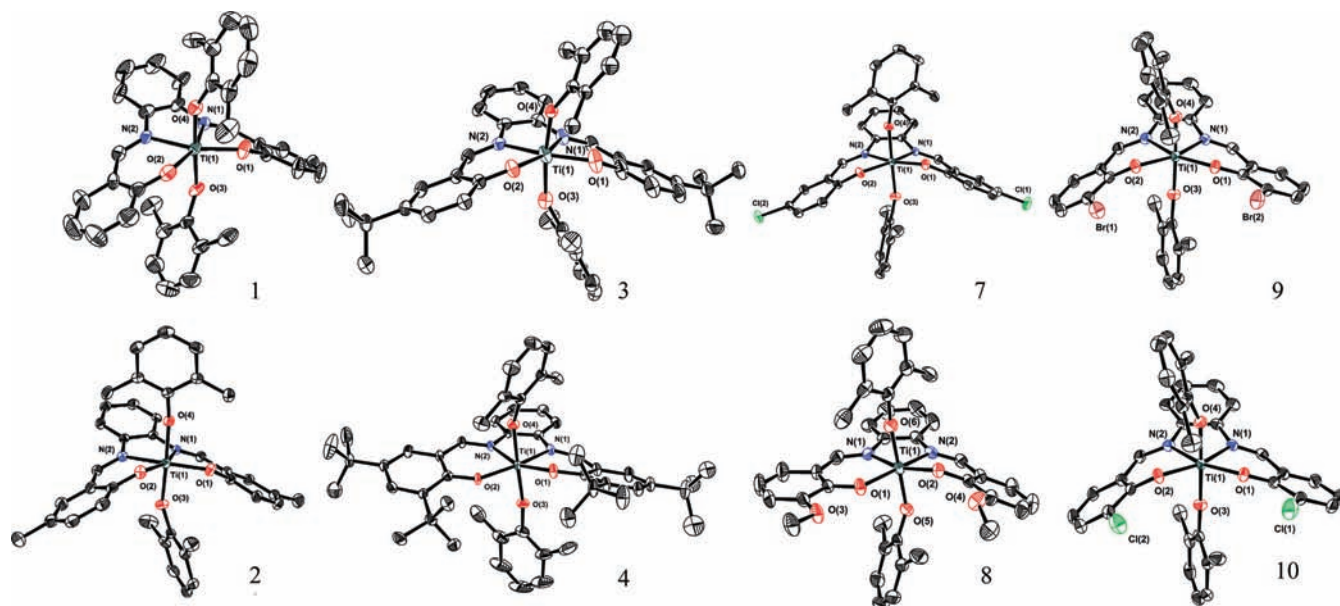


Figure 1. ORTEP drawing of $\text{Lig}^{1-4,7-10}\text{Ti}(\text{OArMe}_2)_2$, depicted as 1–4,7–10, with 50% probability ellipsoids. H atoms were omitted for clarity. For $\text{Lig}^1\text{Ti}(\text{OArMe}_2)_2$, one molecule of the two found in the asymmetric unit is presented. For $\text{Lig}^3\text{Ti}(\text{OArMe}_2)_2$, disorder in the 2,6-dimethylphenolato ligand was omitted for clarity to include only the atoms of 70% occupancy. For $\text{Lig}^4\text{Ti}(\text{OArMe}_2)_2$, disorder in one *t*-Bu group was omitted for clarity. For $\text{Lig}^{9,10}\text{Ti}(\text{OArMe}_2)_2$, dimethylphenol molecule was omitted for clarity.

lengths and angles are provided in Figure 1 and Table S1, Supporting Information, respectively. Compound $\text{Lig}^1\text{Ti}(\text{OArMe}_2)_2$ crystallized with two different molecules in the asymmetric unit, which share similar coordination features. $\text{Lig}^3\text{Ti}(\text{OArMe}_2)_2$ and $\text{Lig}^4\text{Ti}(\text{OArMe}_2)_2$ show disorder in one 2,6-dimethylphenolato ligand and one *tert*-butyl group, respectively, where for the former the main set occurs with 70% occupancy and for the latter 50–50 occupancy is obtained. $\text{Lig}^{9,10}\text{Ti}(\text{OArMe}_2)_2$ crystallized with an accompanying single molecule of 2,6-dimethylphenol each, a product of the reaction of the ligands $\text{H}_2\text{Lig}^{9,10}$ with the precursor $\text{Ti}(\text{OArMe}_2)_4$.

The X-ray structures indicate a similar general geometry of C_{2v} symmetrical complexes with two *trans*-2,6-dimethylphenoxy ligands and with the salphen ligand binding in an equatorial fashion to the octahedral metal center. The Ti–O distances for the phenolato groups are in the range of 1.90–1.94 Å similarly to the analogous values obtained for salan complexes,^{28,29,43–46} while the Ti–N bonds are between 2.15 and 2.17 Å, shorter than the values obtained for the salan analogues due to the sp^2 amine donor. The O–Ti–O angles obtained for all salphen ligands are between 171° and 177°, and O–Ti–O angles for the labile ligands range between 113° and 118°. Thus, it appears that the steric and electronic features of the different substituents induce a relatively small influence on the solid-state structure of the complexes.

Hydrolysis. To estimate and compare the hydrolytic stability of the complexes, ^1H NMR measurements were performed upon addition of 10% D_2O (>1000 equiv relative to Ti) to $\text{THF-}d_8$ solutions of the complexes, as previously described for related salan complexes.^{28,29} These measurements, although not reflecting the exact biological environment, provided a comparative tool to assess the relative stability of the different complexes. The spectrum was measured every 5–10 min for up to 15 h, and integration of selected signals was measured to gain insight on the complexes decomposition process (Figure S1, Supporting Information). In particular, the half-life of dissociation of the 2,6-dimethylphenoxide ligands to give the free 2,6-dimethylphenol was measured by monitoring

the integration of the doublet and triplet signals of the aromatic region and the singlet of the methyl substituents. The results are presented in Table 1 (see also Figure S2 and Table S2,

Table 1. $t_{1/2}$ values for Hydrolysis of the Labile Groups from $\text{Lig}^{1-11}\text{Ti}(\text{OArMe}_2)_2$ at 1:9 $\text{D}_2\text{O}/\text{THF-}d_8$ Solution at Room Temperature Based on Pseudo-First-Order Fit

complex	aromatic substitution	$t_{1/2}$ [h]
$\text{Lig}^1\text{Ti}(\text{OArMe}_2)_2$	none	2
$\text{Lig}^2\text{Ti}(\text{OArMe}_2)_2$	<i>p</i> -Me	3
$\text{Lig}^3\text{Ti}(\text{OArMe}_2)_2$	<i>p</i> - <i>t</i> -Bu	7
$\text{Lig}^4\text{Ti}(\text{OArMe}_2)_2$	<i>o,p</i> -di- <i>t</i> -Bu	5
$\text{Lig}^5\text{Ti}(\text{OArMe}_2)_2$	<i>p</i> -OMe	3
$\text{Lig}^6\text{Ti}(\text{OArMe}_2)_2$	<i>p</i> -Br	4
$\text{Lig}^7\text{Ti}(\text{OArMe}_2)_2$	<i>p</i> -Cl	4
$\text{Lig}^8\text{Ti}(\text{OArMe}_2)_2$	<i>o</i> -OMe	3
$\text{Lig}^9\text{Ti}(\text{OArMe}_2)_2$	<i>o</i> -Br	2
$\text{Lig}^{10}\text{Ti}(\text{OArMe}_2)_2$	<i>o</i> -Cl	11
$\text{Lig}^{11}\text{Ti}(\text{OArMe}_2)_2$	<i>o,p</i> -di-Cl	4
$(\text{bzac})_2\text{Ti}(\text{O}i\text{Pr})_2$		0.5

Supporting Information). Interestingly, no signals corresponding to free salen ligand were detected in the spectra of the hydrolysis products (Figures S1 and S3, Supporting Information), implying that the main product of hydrolysis is a salen-bound oxo-bridged polynuclear compound, as also supported by the crystallographic characterization of such dimeric products obtained for related complexes (Figure S4, Supporting Information).⁴⁷

Complexes $\text{Lig}^{1-2,5-9,11}\text{Ti}(\text{OArMe}_2)_2$ all showed similar stability, with $t_{1/2}$ values for hydrolysis of the labile groups ranging between 2 and 4 h. This stability exceeds that of the known Ti(IV) complex $(\text{bzac})_2\text{Ti}(\text{O}i\text{Pr})_2$ and is comparable to that of some members of the analogous salan family of Ti(IV) complexes.²⁹ $\text{Lig}^3\text{Ti}(\text{OArMe}_2)_2$ and $\text{Lig}^{10}\text{Ti}(\text{OArMe}_2)_2$ demonstrated slightly improved hydrolytic stability with $t_{1/2}$ values

of 7 and 11 h, respectively, the reason of which is not exactly clear as no particular steric or electronic effect stand out for these complexes when compared to other derivatives. Nevertheless, it is obvious that the variation in hydrolytic stability for this series of complexes is relatively minor, supporting the basic chelating salen ligand core as the main contributor to the complexes enhanced stability relative to known compounds. Additionally, this suggests that any variation in the cytotoxicity of these complexes cannot be attributed to hydrolytic stability differences.

Cytotoxicity. Cytotoxic activity was measured on two types of cancer cell lines: colon HT-29 and ovarian OVCAR-1. Analysis was carried out by the methylthiazolyldiphenyl-tetrazolium bromide (MTT) assay following 3 days of incubation with the investigated complexes at different concentrations.²⁸ Relative IC₅₀ and maximal cell growth inhibition values are shown in Table 2. Representative cytotoxicity plots are given in Figure 2.

Table 2. IC₅₀ [μM] and Maximal Cell Growth Inhibition [%] Values of Lig¹⁻¹¹Ti(OArMe₂)₂ and Known Reference Compounds towards HT-29 and OVCAR-1 Cell Lines

complex	aromatic substitution	HT-29 [μM]	OVCAR-1 [μM]
Lig ¹ Ti(OArMe ₂) ₂	none	3.5 ± 0.6 (98%)	3.3 ± 0.5 (98%)
Lig ² Ti(OArMe ₂) ₂	<i>p</i> -Me	10 ± 2 (95%)	9 ± 1 (93%)
Lig ³ Ti(OArMe ₂) ₂	<i>p</i> - <i>t</i> -Bu	4.8 ± 1.1 (60%)	5.2 ± 0.8 (65%)
Lig ⁴ Ti(OArMe ₂) ₂	<i>o</i> , <i>p</i> - <i>di</i> - <i>t</i> -Bu	inactive	inactive
Lig ⁵ Ti(OArMe ₂) ₂	<i>p</i> -OMe	14 ± 4 (83%)	14 ± 3 (80%)
Lig ⁶ Ti(OArMe ₂) ₂	<i>p</i> -Br	2.3 ± 0.6 (96%)	2.1 ± 0.6 (99%)
Lig ⁷ Ti(OArMe ₂) ₂	<i>p</i> -Cl	1.2 ± 0.3 (99%)	1.0 ± 0.3 (100%)
Lig ⁸ Ti(OArMe ₂) ₂	<i>o</i> -OMe	3.9 ± 0.9 (98%)	3.6 ± 0.4 (97%)
Lig ⁹ Ti(OArMe ₂) ₂	<i>o</i> -Br	inactive	inactive
Lig ¹⁰ Ti(OArMe ₂) ₂	<i>o</i> -Cl	inactive	inactive
Lig ¹¹ Ti(OArMe ₂) ₂	<i>o</i> , <i>p</i> - <i>di</i> -Cl	inactive	inactive
reference	HT-29 [μM]	OVCAR-1 [μM]	
cisplatin	20 ± 2 (97%)	13 ± 1 (100%)	
Cp ₂ TiCl ₂	517 ± 87 (100%)	554 ± 120 (100%)	
(bzac) ₂ Ti(OiPr) ₂	11.6 ± 0.8 (99%)	11.5 ± 0.2 (100%)	

When comparing complexes Lig¹⁻⁴Ti(OArMe₂)₂ differing by steric bulk it is clear that reduced steric bulk is preferred for achieving high cytotoxic activity, even where the alkyl substituents are located at the *para* positions. Whereas the *ortho*,*para*-*tert*-butylated complex Lig⁴Ti(OArMe₂)₂ is completely inactive, the *para*-*tert*-butylated complex Lig³Ti(OArMe₂)₂ demonstrates mild activity where maximal cell growth inhibition does not reach over 70%. Maximal inhibition is increased to >70% when decreasing the size of the *para* substituent in the methylated analogue Lig²Ti(OArMe₂)₂, while a further improved performance is detected for Lig¹Ti(OArMe₂)₂, the complex lacking any aromatic alkyl substitutions. This negative influence of general steric bulk, as also observed for analogues,^{28,29} may relate to cell penetration inhibition and/or general hydrophobicity, negatively affecting solubility in biological environment.

Having established that increasing the substituents bulk at various positions negatively affects the cytotoxicity, when examining complexes Lig^{1,5-11}Ti(OArMe₂)₂, a combination of steric and electronic influences at all positions should be taken into account. Complexes Lig^{1,5-7}Ti(OArMe₂)₂ clearly evince

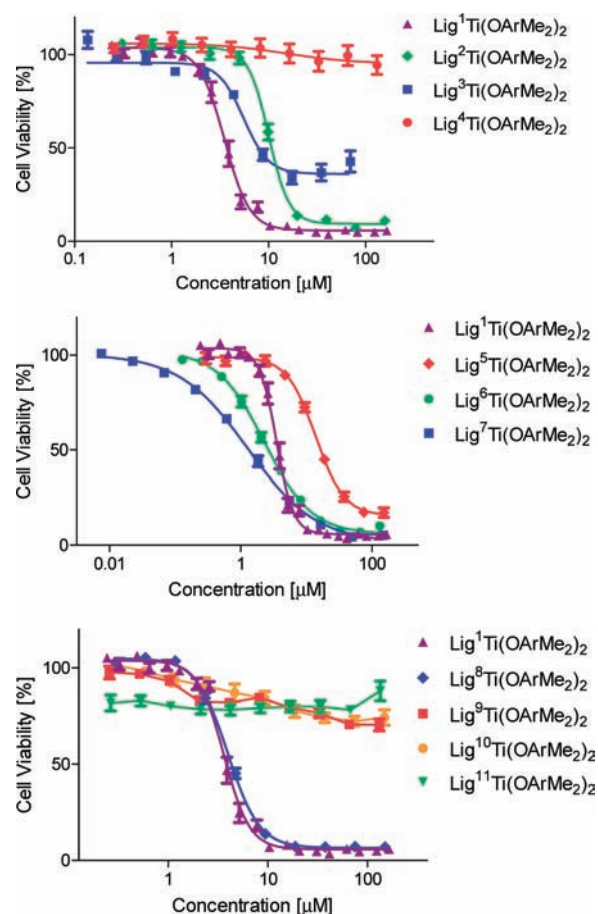


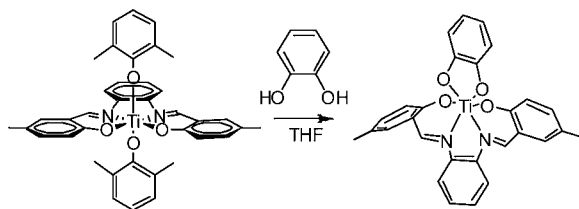
Figure 2. Dependence of HT-29 cell viability based on the MTT assay following a 3-day incubation period on added concentration of Lig¹⁻⁴Ti(OArMe₂)₂ (top), Lig^{1,5-7}Ti(OArMe₂)₂ (middle), and Lig^{1,8-11}Ti(OArMe₂)₂ (bottom) presented on a logarithmic scale.

that *para*-halogenation increases the cytotoxic activity, where the analogous *ortho*-halogenated complexes Lig^{9,10}Ti(OArMe₂)₂ are completely inactive. The *para*-halogenated complexes Lig^{6,7}Ti(OArMe₂)₂ are among the most active members in this series, where the improved performance of the chlorinated one is probably due to reduced steric bulk. In fact, the negative effect of these substitutions at the *ortho* position is more pronounced than their positive effect when located at the *para* position, as may be observed in the inactivity of the *ortho*,*para*-dichlorinated complex Lig¹¹Ti(OArMe₂)₂. Thus, when adding the inactivity of Lig⁴Ti(OArMe₂)₂ to the discussion, one may argue that *ortho* substitutions abolish activity, which may be attributed to (a) interference to the interaction with the biological target, (b) interference to some rearrangement that needs to occur on the metal center upon such interactions, or (c) inhibition to formation of the active species that may be, for instance, some polynuclear hydrolysis product formed in the biological environment. One exception is the *ortho*-methoxylated complex Lig⁸Ti(OArMe₂)₂, demonstrating appreciable cytotoxic activity. It is yet to be determined the reason for which the methoxy substitution leads to different behavior when compared to other derivatives when located both at the *ortho* and at the *para* positions. Possible explanations may relate to the solubility of the complex or conformational changes of the substituent affecting its steric influence.

It is therefore obvious that *trans*-Ti(IV) complexes may indeed be cytotoxic, with activity that exceeds even that of cisplatin by up to ~15-fold on the cell lines analyzed. This raises the question whether the two labile positions interact with the cellular target in an unrelated fashion, rearrangement of the salen ligand occurs on the metal center upon this interaction, or these positions are not at all involved in the activity mechanism.

Analysis of Binding Options. To evaluate whether reorganization on the metal center may occur upon the first interaction of the complexes with a suitable target to form a chelate binding, we reacted a representative complex with a strong chelating bidentate ligand. $\text{Lig}^2\text{Ti}(\text{OArMe}_2)_2$ was reacted with 1 equiv of *ortho*-catechol in THF at room temperature under an inert atmosphere. Complex $\text{Lig}^2\text{Ti}(\text{O}_2\text{Ar})$ thus formed (Scheme 2), for which the ^1H and ^{13}C NMR analyses

Scheme 2



revealed a single type of aromatic phenolato system and a single set of the *ortho*-catechol ligand signals. Crystallization from dichloromethane at room temperature yielded single red crystals suitable for X-ray crystallography. An ORTEP drawing of the complex $\text{Lig}^2\text{Ti}(\text{O}_2\text{Ar})$ is presented in Figure 3, and a list of selected bond lengths and angles is given in Table 3.

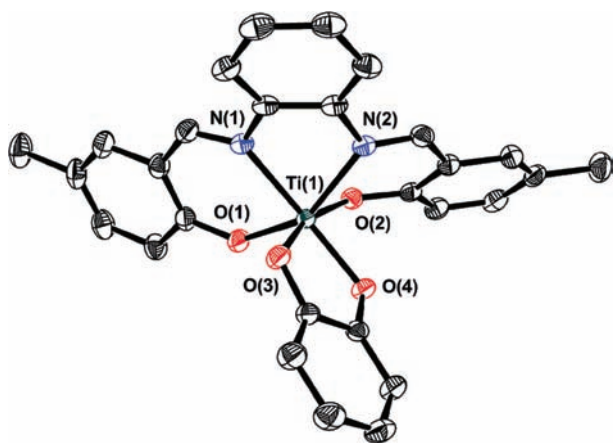


Figure 3. ORTEP drawing of $\text{Lig}^2\text{Ti}(\text{O}_2\text{Ar})$ with 50% probability ellipsoids. H atoms and dichloromethane solvent were omitted for clarity.

The X-ray structure evinces that the catecholato ligand binds to the metal in a bidentate chelating fashion, where rearrangement of the salen ligand occurred to enable the *cis* configuration of what used to be the labile ligands, while the salen ligand is no longer equatorial, adopting a *cis* configuration of the phenolato moieties. In fact, this C_1 -symmetrical structure highly resembles that obtained for an analogous catecholato salan complex following reaction of the bis(isopropoxo) precursor with *o*-catechol, where the phenolato binding

Table 3. Selected Bond Lengths [Angstroms] and Angles [degrees] for $\text{Lig}^2\text{Ti}(\text{O}_2\text{Ar})$

atoms	value	atoms	value
lengths			
O(1)–Ti	1.886(2)	N(1)–Ti	2.146(2)
O(2)–Ti	1.880(2)	N(2)–Ti	2.184(2)
O(3)–Ti	1.937(2)		
O(4)–Ti	1.938(2)		
angles			
O(1)–Ti–O(2)	92.19(7)	O(1)–Ti–N(1)	82.06(7)
O(1)–Ti–O(3)	84.17(6)	O(2)–Ti–N(1)	149.76(7)
O(1)–Ti–O(4)	162.22(6)	O(3)–Ti–N(1)	99.00(7)
O(2)–Ti–O(3)	109.97(7)	O(4)–Ti–N(1)	94.87(7)
O(2)–Ti–O(4)	98.88(7)	O(1)–Ti–N(2)	115.00(6)
O(3)–Ti–O(4)	79.01(6)	O(2)–Ti–N(2)	83.02(7)
N(1)–Ti–N(2)	72.87(7)	O(3)–Ti–N(2)	157.05(6)
		O(4)–Ti–N(2)	80.34(6)

changed from a *trans* to a *cis* orientation.²⁹ This result is in agreement with the notion that reorganization of the ligand on the metal center may occur where a strong chelating target is introduced and also supports similar interaction for both the salen and the salen families of complexes due to relatively high flexibility of the octahedral metal center. Interestingly, as occurred for the salan analogue²⁹ and despite the reduced lability, the catecholato complex exhibits appreciable cytotoxic activity as well, with IC_{50} values of 16 ± 5 and $15 \pm 5 \mu\text{M}$ for HT-29 and OVCAR-1 cell lines, respectively, that are similar to the values of the *trans* analog $\text{Lig}^2\text{Ti}(\text{OArMe}_2)_2$. This raises the additional possibility that the labile positions do not participate directly as such in the cytotoxicity mechanism if, for instance, an oxo-bridged polynuclear hydrolysis product is involved as the active species. The catecholato complex also demonstrates, as expected,²⁹ increased hydrolytic stability where no substantial catecholato hydrolysis is observed for days in 10% D_2O solutions.

Hydrolysis Effect on Cytotoxicity. To further analyze the relationship between hydrolysis and cytotoxicity and especially as a similar hydrolysis rate was detected for complexes of varying activities, we reinvestigated the cytotoxic activity of the most active complex $\text{Lig}^7\text{Ti}(\text{OArMe}_2)_2$ following varying periods of preincubation in the biological medium without cells. Thus, $\text{Lig}^7\text{Ti}(\text{OArMe}_2)_2$ was exposed to the medium for 0, 1, 3, and 24 h of incubation, following which cells were added for an additional 3 days of incubation and the viability was measured. Figure 4 depicts the results obtained for $\text{Lig}^7\text{Ti}(\text{OArMe}_2)_2$ toward HT-29 cells, while Figure 5 depicts the cell viability recorded following 3 h of preincubation in comparison to the results obtained for $(\text{bzac})_2\text{Ti}(\text{OiPr})_2$ and for an analogous *meta-para*-alkylated salan complex of similar stability in 10% D_2O ⁴⁸ ($t_{1/2}$ for isopropoxo hydrolysis of 5 h²⁹). As no activity was recorded for $(\text{bzac})_2\text{Ti}(\text{OiPr})_2$ following 24 h of medium preincubation, Figure 6 depicts the results for these measurements for the salen and salan complexes only. IC_{50} values are provided in Table 4.

The results depicted in Figure 4 reveal that although cytotoxicity markedly decreases following preincubation in biological medium which should probably be attributed to some dissociation of the complex, appreciable activity is retained even after 24 h of medium preincubation. Additionally, higher sustainability of the activity is observed for the salen complex in comparison to known Ti(IV) complexes: $(\text{bzac})_2\text{Ti}(\text{OiPr})_2$ loses all activity already following 3 h of medium

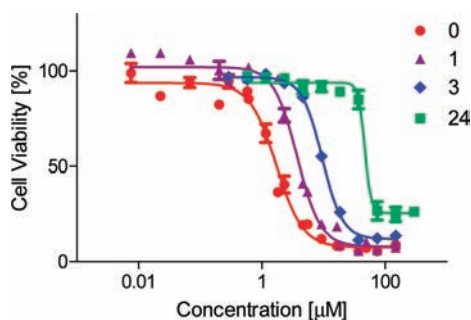


Figure 4. Dependence of HT-29 cell viability on administered concentration of $\text{Lig}^7\text{Ti}(\text{OArMe}_2)_2$ following preincubation in aqueous medium for varying periods (given in hours) prior to cell addition and 3 days incubation with cells. Presented on a logarithmic scale.

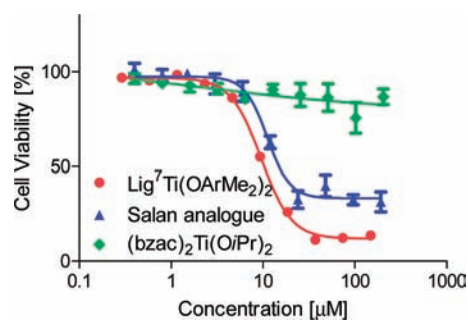


Figure 5. Dependence of HT-29 cell viability on administered concentration of $\text{Lig}^7\text{Ti}(\text{OArMe}_2)_2$, $(\text{bzac})_2\text{Ti}(\text{OiPr})_2$,⁴⁸ and a *meta,para*-alkylated salan analogue⁴⁸ following 3 h preincubation in aqueous medium prior to cell addition and 3 days incubation with cells. Presented on a logarithmic scale.

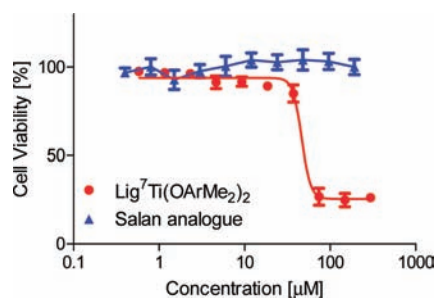


Figure 6. Dependence of HT-29 cell viability on administered concentration of $\text{Lig}^7\text{Ti}(\text{OArMe}_2)_2$ and a *meta,para*-alkylated salan analogue⁴⁸ following 24 h preincubation in aqueous medium prior to cell addition and 3 days incubation with cells. Presented on a logarithmic scale.

Table 4. IC_{50} [μM] and Maximal Cell Growth Inhibition [%] Values of $\text{Lig}^7\text{Ti}(\text{OArMe}_2)_2$ Following Preincubation in Aqueous Medium for Varying Periods [hours] Prior to Cell Addition and 3 Days Incubation with Cells

preincubation [h]	HT-29 [μM]	OVCAR-1 [μM]
0	1.7 \pm 0.4 (93%)	1.7 \pm 0.3 (91%)
1	3.9 \pm 0.5 (92%)	3.9 \pm 0.2 (91%)
3	9.5 \pm 0.9 (88%)	9.2 \pm 0.6 (89%)
24	43 \pm 15 (74%)	45 \pm 18 (70%)

preincubation where both the salan and salen complexes are still notably active (Figure 5), while the salan analogue is

inactive following 24 h of medium preincubation (Figure 6). Assuming that a polynuclear hydrolysis product should readily form under these conditions, it appears that such an oxo-bridged salen cluster might itself be cytotoxic, where activity decrease may be attributed to reduced solubility and precipitation and/or to impaired cellular penetration capability of the larger molecule.

CONCLUSIONS

In this study we discussed the first family of anticancer *trans*-Ti(IV) complexes to be reported, which is based on salophen ligands. Such ligands have previously been shown to lead to highly cytotoxic complexes of other transition metals as well, such as iron(III) and manganese(III).^{49–52} Additionally, complexes of the Ti(IV)–salen family demonstrate hydrolytic stability comparable to that of some alkylated analogues of the salan family,²⁹ with cytotoxic activity markedly higher than that of cisplatin. Structure–activity relationship investigations revealed that while aromatic substitutions have a minor effect on the hydrolytic stability, they strongly influence the cytotoxic properties of the complexes. Overall, we observed that reduced steric bulk is favored, *ortho*-substitution mostly abolished the activity, while *para*-halogenation produced the most active complexes of this family.

When compared to analogous salan complexes,^{28,29} the effects of geometry, substitutions, and hydrolysis are quite intriguing. It appears that a similar mechanism may involve the activity of the two groups of complexes, as reaction with catechol of both the bis(isopropoxo) salan–Ti(IV) and the bis(dimethylphenolato) salen–Ti(IV) precursors yielded catecholato complexes of highly similar geometry and cytotoxic activity.²⁹ Thus, similar reorganizations may occur upon interaction with a chelating cellular target due to the higher flexibility of the octahedral metal center than that of, for instance, the square planar platinum compounds. It is possible that for this reason *ortho*-halogenation affects differently the salan and salen families of complexes: whereas salan complexes become more active and stable,²⁸ the salen compounds are inactive, perhaps due to interference to the required reorganization. An alternative mechanistic route may relate to the activity and properties of the hydrolysis products, presumed to be oxo-bridged salen-bound polynuclear compounds. As the salen complexes retain notable cytotoxic activity after periods of preincubation in water that largely exceed their $t_{1/2}$ of labile ligand hydrolysis in 10% D₂O solution, it is certainly plausible that polynuclear hydrolysis products might not only be somewhat active themselves but may also exhibit some membrane penetration ability. Such characteristics seem to be lacking for the salan analogues,^{29,53,54} as the isolated clusters lack cytotoxicity altogether, although their involvement in the cytotoxicity mechanism when formed inside the cells has previously been proposed.^{53–55} One possible reason for this difference may relate to different sizes of the clusters, if indeed dimeric, rather than trimeric salen-bound clusters are involved. The activity of the stable hydrolysis products is certainly advantageous since reduced hydrolysis concerns should allow for longer shelf-lives of the compounds. Nevertheless, as the activity of the salens clearly decreases following water exposure, additional derivatives with increased solubility should be analyzed in order to make such clusters of potential medicinal use. Additional advantages of the salen complexes relate to the lack of chirality that abolished the need for chiral separation for applicability as occurs for the salan complexes^{53,55,56} and in

Table 5. Crystal Data for Lig^{1-4,8,9}Ti(OArMe₂)₂^a and Lig²Ti(O₂Ar)

parameter/ compound ^a	1	2	3	4	8	9	Lig ² Ti(O ₂ Ar)
formula	C ₃₆ H ₃₂ N ₂ O ₄ Ti	C ₃₈ H ₃₆ N ₂ O ₄ Ti	C ₄₄ H ₄₈ N ₂ O ₄ Ti	C ₅₂ H ₆₄ N ₂ O ₄ Ti	C ₃₈ H ₃₆ N ₂ O ₆ Ti	C ₃₆ H ₃₀ Br ₂ N ₂ O ₄ Ti·C ₈ H ₁₀ O	C ₂₈ H ₂₂ N ₂ O ₄ Ti·CH ₂ Cl ₂
M _w	604.54	632.59	716.74	828.95	664.59	884.50	583.30
space group	P2 ₁ /n	P2 ₁ /n	P2 ₁ /c	P2 ₁ /c	Cc	P2 ₁ /c	P-1
a [Å]	22.886(4)	13.1517(9)	9.104(4)	13.656(1)	13.372(1)	11.673(1)	8.877(3)
b [Å]	9.457(2)	14.281(1)	26.33(1)	18.749(1)	23.313(4)	19.951(2)	9.769(3)
c [Å]	29.041(6)	16.989(1)	17.051(7)	18.542(1)	12.053(2)	17.293(2)	16.796(5)
α [deg]							93.968(5)
β [deg]	100.420(3)	100.437(1)	101.481(7)	99.331(1)	117.448(3)	105.846(2)	106.103(3)
γ [deg]							109.979(5)
V [Å ³]	6181(2)	3138.0(4)	4004(3)	4684.9(6)	3334.2(9)	3874.3(6)	1307.6(7)
T [K]	173(1)	173(1)	123(1)	173(1)	173(2)	173(1)	173(1)
Z	8	4	4	4	4	4	2
μ(Mo Kα) [mm ⁻¹]	0.319	0.317	0.256	0.228	0.306	2.333	0.571
no. of reflns measd	66 071	34 149	44 124	50 477	19 307	44 147	14 979
no. of reflns unique	13 460	6828	8748	10 217	7797	9220	6024
R _{int}	0.1312	0.0766	0.0498	0.0960	0.0500	0.0418	0.0246
R(F _o ²) for [I > 2σ(I)]	0.1397	0.0707	0.0837	0.1028	0.0625	0.0375	0.0483
R _w for [I > 2σ(I)]	0.2368	0.1399	0.2176	0.1846	0.1135	0.0845	0.1186

^aCompounds 1–4, 8, and 9 represent Lig^{1-4,8,9}Ti(OArMe₂)₂, respectively. For Lig^{7,10}Ti(OArMe₂)₂ see ref 34.

their enhanced solubility in biologically relevant solvents, such as DMSO. Studies currently underway with these highly promising anticancer complexes include the detailed investigation of their mechanism of action to identify the active species and its relation to the hydrolysis processes.

EXPERIMENTAL SECTION

For H₂Lig^{1,2,7,10} and Lig^{1,2,7,10}Ti(OArMe₂)₂ see our previous communication.³⁴ Syntheses of ligands H₂Lig^{3-6,8,11} were achieved as previously described starting from the commercially available substituted salicylaldehyde.⁵⁷⁻⁶² 1,2-Diaminobenzene (99.5%), 3-bromo-2-hydroxybenzaldehyde (97%), and pyrocatechol (99%) were purchased from Sigma Aldrich Chemical Co. Inc. and used without further purification. Ti(OArMe₂)₄ was synthesized as previously described.⁴² All solvents used for procedures requiring an inert atmosphere were either distilled from potassium or potassium/benzophenone under nitrogen or dried over alumina columns on a M. Braun SPS-800 solvent purification system. All experiments requiring dry atmosphere were performed in an M. Braun drybox under nitrogen atmosphere or using Schlenk line techniques. NMR data were recorded using an AMX-500 MHz Bruker spectrometer. CDCl₃ (99.8%) was purchased from Cambridge Isotope Laboratories Inc. and used without further purification. X-ray diffraction data were obtained with a Bruker Smart Apex diffractometer, running the SMART software package. After collection, the raw data frames were integrated by the SAINT software package. The structures were solved and refined using the SHELXTL software package. Crystal data for Lig^{1-4,8,9}Ti(OArMe₂)₂ and Lig²Ti(O₂Ar) are summarized in Table 5.³⁴

Elemental analyses were performed in the microanalytical laboratory in our institute. Accurate-Mass Q-TOF LC/MS measurements were carried on an Agilent Technologies 6520. Cytotoxicity was measured on HT-29 colon and OVCAR-1 ovarian cancer cells obtained from ATCC Inc. using the methylthiazolyldiphenyltetrazolium bromide (MTT) assay as previously described,²⁸ starting from 0.9 × 10⁶ cells, incubated with the complexes at different concentrations for 3 days, where each measurement was repeated at least 3 × 3 times. (Bzac)₂Ti(OiPr)₂ was administered in THF as were all salen complexes under general study, while the reference compounds cisplatin and Cp₂TiCl₂ were administered in DMSO. Relative IC₅₀ values were determined by a nonlinear regression of a variable slope (four parameters) model. Measurements relating to the effect of

medium exposure were conducted similarly, following preincubation of the complex with the medium at 37 °C for 1, 3, and 24 h, where the compound Lig⁷Ti(OArMe₂)₂ was administered in DMSO. Kinetic studies by NMR to monitor hydrolysis of dimethylphenolato groups to give polynuclear products (Figure S1, Supporting Information), for establishment of relative water resistance, were performed as previously described^{28,29} using ca. 6 mM of the complex solution in d₈-THF and adding D₂O to give a final solution of 1:9 D₂O/d₈-THF with added D₂O being >1000 equiv relative to Ti(IV). The t_{1/2} value is based on a pseudo-first-order fit for each compound (Figure S2, Supporting Information, all R² fit values ≥ 0.98), as the average of values obtained for several signals of the labile ligands. The results were verified by including *p*-dinitro benzene as an internal standard. The sum of integration of (CH₃)₂C₆H₃O–Ti and (CH₃)₂C₆H₃OH in the first measurement following D₂O addition was assigned as integration 1. Characterization of hydrolysis products was further conducted by reacting selected complexes with 10 000 equiv of water for 3 days, removing the volatiles, washing with hexane, and dissolving the product in DMSO-*d*₈ for ¹H NMR analysis (Figure S3, Supporting Information).

H₂Lig⁹. 1,2-Diaminophenol (0.27 g, 2.50 mmol) dissolved in methanol was added to 3-bromosalicylaldehyde (1.00 g, 5.0 mmol) dissolved in methanol. The solution was stirred at reflux for 3 h. The solution was then cooled to give an orange precipitate, which was collected by vacuum filtration and dried in vacuo, giving H₂Lig⁹ (84%). Anal. Calcd for C₂₀H₁₄Br₂N₂O₂: C, 50.66; H, 2.98; N, 5.91. Found: C, 50.69; H, 2.64; N, 5.93. ¹H NMR (500 MHz; CDCl₃) 13.71 (2H, s, OH), 8.59 (2H, s, CH), 7.63 (2H, dd, *J* = 7.5, 1.5 Hz, Ar), 7.36 (4H, m, Ar), 7.22 (2H, m, Ar), 6.83 (2H, t, *J* = 7.5 Hz, Ar). ¹³C NMR (125 MHz; CDCl₃) 163.8, 158.2, 141.9, 136.9, 131.8, 128.2, 120.7, 120.2, 119.9, 111.5.

Lig³Ti(OArMe₂)₂. Lig³Ti(OArMe₂)₂ was synthesized in analogy to Lig^{1,2,4,10}Ti(OArMe₂)₂³⁴ from Ti(OArMe₂)₄ (100 mg, 0.19 mmol) and H₂Lig³ (81 mg, 0.19 mmol) (73%). Anal. Calcd for C₄₄H₄₈N₂O₄Ti: C, 73.73; H, 6.75; N, 3.91. Found: C, 73.22; H, 6.47; N, 3.78. ¹H NMR (500 MHz; CDCl₃) 8.64 (2H, s, CH), 7.57 (2H, m, Ar), 7.41 (2H, dd, *J* = 9.0, 2.5 Hz, Ar), 7.39 (2H, m, Ar), 7.27 (2H, d, *J* = 2.5 Hz, Ar), 6.67 (2H, d, *J* = 9.0 Hz, Ar), 6.60 (4H, d, *J* = 7.5 Hz, Ar), 6.33 (2H, t, *J* = 7.5 Hz, Ar), 1.97 (12H, s, CH₃), 1.26 (18H, s, CH₃). ¹³C NMR (125 MHz; CDCl₃) 164.4, 164.3, 143.1, 141.1, 135.5, 131.1, 129.2, 128.8, 127.6, 126.0, 122.3, 118.5, 117.5, 117.1, 34.1, 31.3, 17.4.

Lig⁴Ti(OArMe)₂. Lig⁴Ti(OArMe)₂ was synthesized similarly from Ti(OArMe)₂ (100 mg, 0.19 mmol) and H₂Lig⁴ (102 mg, 0.19 mmol). The crude product was washed several times with dry hexane to give the red product (58%). Anal. Calcd for C₅₂H₆₄N₂O₄Ti: C, 75.34; H, 7.78; N, 3.38. Found: C, 74.74; H, 7.56; N, 3.27. ESI-HRMS (C₅₂H₆₄N₂O₄Ti + Na) *m/z* Calcd: 851.4238. [M⁺Na⁺] Found: 851.4242. ¹H NMR (500 MHz; CDCl₃) 8.62 (2H, s, CH), 7.57 (2H, d, *J* = 2.5 Hz, Ar), 7.48 (2H, m, Ar), 7.30 (2H, m, Ar), 7.17 (2H, d, *J* = 2.5 Hz, Ar), 6.58 (4H, d, *J* = 7.5 Hz, Ar), 6.35 (2H, t, *J* = 7.5 Hz, Ar), 1.78 (12H, s, CH₃), 1.46 (18H, s, CH₃), 1.32 (18H, s, CH₃). ¹³C NMR (125 MHz; CDCl₃) 164.5, 163.8, 159.5, 142.9, 140.6, 137.3, 132.8, 129.5, 128.9, 127.7, 126.3, 123.7, 118.2, 116.7, 35.7, 34.3, 31.5, 30.2, 17.8.

Lig⁵Ti(OArMe)₂. Lig⁵Ti(OArMe)₂ was synthesized similarly from Ti(OArMe)₂ (100 mg, 0.19 mmol) and H₂Lig⁵ (71 mg, 0.19 mmol) (78%). ¹H NMR (500 MHz; CDCl₃) 8.59 (2H, s, CH), 7.54 (2H, m, Ar), 7.39 (2H, m, Ar), 7.02 (2H, dd, *J* = 9.0, 3.0 Hz, Ar), 6.80 (2H, d, *J* = 3.0 Hz, Ar), 6.69 (2H, d, *J* = 9.0 Hz, Ar), 6.62 (4H, d, *J* = 7.5 Hz, Ar), 6.36 (2H, t, *J* = 7.5 Hz, Ar), 3.74 (6H, s, CH₃), 1.97 (12H, s, CH₃). ¹³C NMR (125 MHz; CDCl₃) 164.3, 161.6, 159.1, 151.9, 129.5, 128.8, 127.6, 126.5, 126.0, 122.2, 118.9, 118.5, 117.1, 116.2, 56.1, 17.4.

Lig⁶Ti(OArMe)₂. Lig⁶Ti(OArMe)₂ was synthesized similarly from Ti(OArMe)₂ (100 mg, 0.19 mmol) and H₂Lig⁶ (89 mg, 0.19 mmol) (72%). Anal. Calcd for C₃₆H₃₀Br₂N₂O₄Ti: C, 56.72; H 3.97; N, 3.67. Found: C, 56.42; H, 3.94; N, 3.59. ¹H NMR (500 MHz; CDCl₃) 8.57 (2H, s, CH), 7.55 (2H, m, Ar), 7.49 (2H, d, *J* = 3.0 Hz, Ar), 7.45 (2H, m, Ar), 7.41 (2H, dd, *J* = 9.0, 2.5 Hz, Ar), 6.66 (2H, d, *J* = 9.0 Hz, Ar), 6.64 (4H, d, *J* = 7.5 Hz, Ar), 6.41 (2H, t, *J* = 7.5 Hz, Ar), 1.95 (12H, s, CH₃). ¹³C NMR (125 MHz; CDCl₃) 165.1, 164.1, 158.6, 142.8, 140.0, 136.8, 130.1, 127.8, 126.0, 124.1, 120.0, 119.3, 117.3, 109.9, 17.3.

Lig⁸Ti(OArMe)₂. Lig⁸Ti(OArMe)₂ was synthesized similarly from Ti(OArMe)₂ (100 mg, 0.19 mmol) and H₂Lig⁸ (71 mg, 0.19 mmol) (75%). Anal. Calcd for C₃₈H₃₆N₂O₆Ti: C, 68.68; H, 5.46; N, 4.22. Found: C, 68.74; H, 5.24; N, 4.17. ¹H NMR (500 MHz; CDCl₃) 8.64 (2H, s, CH), 7.53 (2H, m, Ar), 7.39 (2H, m, Ar), 6.98 (2H, dd, *J* = 8.0, 1.5 Hz, Ar), 6.91 (2H, dd, *J* = 8.0, 1.5 Hz, Ar), 6.63 (2H, t, *J* = 7.5 Hz, Ar), 6.61 (4H, d, *J* = 7.5 Hz, Ar), 6.35 (2H, t, *J* = 7.5 Hz, Ar), 3.83 (6H, s, CH₃), 2.01 (12H, s, CH₃). ¹³C NMR (125 MHz; CDCl₃) 164.4, 159.8, 157.8, 149.0, 143.1, 129.4, 127.4, 126.8, 126.5, 123.1, 118.8, 118.6, 118.0, 117.1, 56.6, 17.2.

Lig⁹Ti(OArMe)₂. Lig⁹Ti(OArMe)₂ was synthesized similarly from Ti(OArMe)₂ (100 mg, 0.19 mmol) and H₂Lig⁹ (89 mg, 0.19 mmol) (81%). Anal. Calcd for C₃₆H₃₀Br₂N₂O₄Ti: C, 56.72; H, 3.97; N, 3.67. Found: C, 56.59; H, 3.95; N, 3.59. ¹H NMR (500 MHz; CDCl₃) 8.69 (2H, s, CH), 7.66 (2H, dd, *J* = 8.0, 1.5 Hz, Ar), 7.61 (2H, m, Ar), 7.50 (2H, m, Ar), 7.33 (2H, dd, *J* = 7.5, 1.5 Hz, Ar), 6.67 (4H, d, *J* = 7.5 Hz, Ar), 6.59 (2H, t, *J* = 7.5 Hz, Ar), 6.41 (2H, t, *J* = 7.5 Hz, Ar), 2.07 (12H, s, CH₃). ¹³C NMR (125 MHz; CDCl₃) 164.1, 162.6, 160.2, 143.1, 140.5, 134.7, 130.0, 127.7, 126.3, 123.1, 119.2, 119.1, 117.4, 113.2, 17.7.

Lig¹¹Ti(OArMe)₂. Lig¹¹Ti(OArMe)₂ was synthesized similarly from Ti(OArMe)₂ (100 mg, 0.19 mmol) and H₂Lig¹¹ (85 mg, 0.19 mmol) (71%). Anal. Calcd for C₃₆H₂₈Cl₄N₂O₄Ti: C, 58.25; H, 3.80; N, 3.77. Found: C, 58.25; H, 3.40; N, 3.75. ¹H NMR (500 MHz; CDCl₃) 8.62 (2H, s, CH), 7.60 (2H, m, Ar), 7.57 (2H, m, Ar), 7.45 (2H, d, *J* = 2.5 Hz, Ar), 7.27 (2H, d, *J* = 2.5 Hz, Ar), 6.68 (4H, d, *J* = 7.5 Hz, Ar), 6.45 (2H, t, *J* = 7.5 Hz, Ar), 2.02 (12H, s, CH₃). ¹³C NMR (125 MHz; CDCl₃) 164.0, 160.6, 159.2, 142.9, 136.7, 132.3, 130.6, 128.8, 127.9, 126.2, 124.5, 123.3, 122.3, 119.7, 17.4.

Lig²Ti(O₂Ar). Lig²Ti(OArMe)₂ (100 mg, 0.158 mmol) in dry THF was stirred until dissolution was achieved. Pyrocatechol (17 mg, 0.16 mmol) dissolved in dry THF was added. The solution was left overnight at room temperature under a nitrogen atmosphere. The crude product was washed several times with dry diethyl ether to give the dark red product (87%). Anal. Calcd for C₂₈H₂₂N₂O₄Ti·2/3CH₂Cl₂: C, 62.04; H, 4.24; N, 5.05. Found: C, 62.12; H, 4.53; N, 4.60. ESI-HRMS (C₂₈H₂₂N₂O₄Ti + H) Calcd: 499.1132. [M⁺H⁺] Found: 499.1147. ¹H NMR (500 MHz; CDCl₃) 8.80 (2H, s, CH), 7.62 (2H, m, Ar), 7.41 (4H, m, Ar), 7.33 (2H, d, *J* = 1.5 Hz, Ar), 7.06 (2H, d, *J* = 8.0 Hz, Ar), 6.43 (2H, m, Ar), 6.07 (2H, m, Ar), 2.35 (6H, s, CH₃)

¹³C NMR (125 MHz; CDCl₃) 162.5, 160.4, 160.0, 143.9, 138.5, 133.6, 129.9, 129.0, 122.6, 119.3, 118.6, 117.0, 110.7, 20.6. Following solution of the X-ray structure, remeasuring the unit cell parameters of additional crystals, and redetermining their ¹H NMR confirmed that the solved structure corresponds to the main product.

■ ASSOCIATED CONTENT

Supporting Information

Crystallographic data, representative spectra and plots of hydrolysis, spectra of representative hydrolysis products and related structures, and plots of cytotoxicity toward OVCAR-1 cells. This material is available free of charge via the Internet at <http://pubs.acs.org>.

■ AUTHOR INFORMATION

Corresponding Author

*E-mail: tshuva@chem.ch.huji.ac.il.

■ ACKNOWLEDGMENTS

We thank Dr. Shmuel Cohen for crystallographic analyses. This research received funding from the European Research Council under the European Community's Seventh Framework Programme (FP7/2007-2013)/ERC Grant agreement no. 239603.

■ REFERENCES

- (1) Abu-Surrah, A. S.; Kettunen, M. *Curr. Med. Chem.* **2006**, *13*, 1337–1357.
- (2) Barnes, K. R.; Lippard, S. J. *Met. Ions Biol. Syst.* **2004**, *42*, 143–177.
- (3) Wong, E.; Giandomenico, C. M. *Chem. Rev.* **1999**, *99*, 2451–2466.
- (4) Cepeda, V.; Fuertes, M. A.; Castilla, J.; Alonso, C.; Quevedo, C.; Perez, J. M. *Anti-Cancer Agents Med. Chem.* **2007**, *7*, 3–18.
- (5) Garbutcheon-Singh, K. B.; Grant, M. P.; Harper, B. W.; Krause-Heuer, A. M.; Manohar, M.; Orkey, N.; Aldrich-Wright, J. R. *Curr. Top. Med. Chem.* **2011**, *11*, 521–542.
- (6) Buijninx, P. C. A.; Sadler, P. J. *Curr. Opin. Chem. Biol.* **2008**, *12*, 197–206.
- (7) Desoize, B. *Anticancer Res.* **2004**, *24*, 1529–1544.
- (8) Galanski, M.; Arion, V. B.; Jakupec, M. A.; Keppler, B. K. *Curr. Pharm. Des.* **2003**, *9*, 2078–2089.
- (9) Jakupec, M. A.; Galanski, M.; Arion, V. B.; Hartinger, C. G.; Keppler, B. K. *Dalton Trans.* **2008**, 183–194.
- (10) Ott, I.; Gust, R. *Arch. Pharm. Chem. Life Sci.* **2007**, *340*, 117–126.
- (11) van Rijt, S. H.; Sadler, P. J. *Drug Discovery Today* **2009**, *14*, 1089–1097.
- (12) Xu, D. R.; Cui, Y. B.; Cui, K.; Gou, S. H. *Prog. Chem.* **2006**, *18*, 107–113.
- (13) Clarke, M. J.; Zhu, F.; Frasca, D. R. *Chem. Rev.* **1999**, *99*, 2511–2543.
- (14) Köpf-Maier, P. *Eur. J. Clin. Pharmacol.* **1994**, *47*, 1–16.
- (15) Kratz, F.; Schutte, M. T. *Cancer J.* **1998**, *11*, 176–182.
- (16) Abeyasinghe, P. M.; Harding, M. M. *Dalton Trans.* **2007**, 3474–3482.
- (17) Caruso, F.; Rossi, M. *Mini-Rev. Med. Chem.* **2004**, *4*, 49–60.
- (18) Caruso, F.; Rossi, M.; Pettinari, C. *Expert Opin. Ther. Patents* **2001**, *11*, 969–979.
- (19) Christodoulou, C. V.; Eliopoulos, A. G.; Young, L. S.; Hodgkins, L.; Ferry, D. R.; Kerr, D. J. *Br. J. Cancer* **1998**, *77*, 2088–2097.
- (20) Kelter, G.; Sweeney, N. J.; Strohfeldt, K.; Fiebig, H.-H.; Tacke, M. *Anti-Cancer Drugs* **2005**, *16*, 1091–1098.
- (21) Keppler, B. K.; Friesen, C.; Moritz, H. G.; Vongerichten, H.; Vogel, E. *Struct. Bonding (Berlin)* **1991**, *78*, 97–127.
- (22) Köpf-Maier, P.; Köpf, H. *Chem. Rev.* **1987**, *87*, 1137–1152.

- (23) Köpf-Maier, P.; Köpf, H. *Struct. Bonding (Berlin)* **1988**, *70*, 103–185.
- (24) Meléndez, E. *Crit. Rev. Oncol. Hematol.* **2002**, *42*, 309–315.
- (25) Strohfeldt, K.; Tacke, M. *Chem. Soc. Rev.* **2008**, *37*, 1174–1187.
- (26) Caruso, F.; Massa, L.; Gindulyte, A.; Pettinari, C.; Marchetti, F.; Pettinari, R.; Ricciutelli, M.; Costamagna, J.; Canales, J. C.; Tanski, J.; Rossi, M. *Eur. J. Inorg. Chem.* **2003**, 3221–3232.
- (27) Toney, J. H.; Marks, T. J. *J. Am. Chem. Soc.* **1985**, *107*, 947–953.
- (28) Peri, D.; Meker, S.; Manna, C. M.; Tshuva, E. Y. *Inorg. Chem.* **2011**, *50*, 1030–1038.
- (29) Peri, D.; Meker, S.; Shavit, M.; Tshuva, E. Y. *Chem.—Eur. J.* **2009**, *15*, 2403–2415.
- (30) Shavit, M.; Peri, D.; Manna, C. M.; Alexander, J. S.; Tshuva, E. Y. *J. Am. Chem. Soc.* **2007**, *129*, 12098–12099.
- (31) Tshuva, E. Y.; Ashenurst, J. A. *Eur. J. Inorg. Chem.* **2009**, 2203–2218.
- (32) Tshuva, E. Y.; Peri, D. *Coord. Chem. Rev.* **2009**, *253*, 2098–2115.
- (33) Aris, S. M.; Farrell, N. P. *Eur. J. Inorg. Chem.* **2009**, 1293–1302.
- (34) Tzuberly, A.; Tshuva, E. Y. *Inorg. Chem.* **2011**, *50*, 7946–7948.
- (35) Chen, H.; White, P. S.; Gange, M. R. *Organometallics* **1998**, *17*, 5358–5366.
- (36) Solari, E.; Floriani, C.; Chiesi-Villa, A.; Rizzoli, C. *J. Chem. Soc., Dalton Trans.* **1992**, 367–373.
- (37) Khandar, A. A.; Shaabani, B.; Belaj, F.; Bakhtiari, A. *Inorg. Chim. Acta* **2007**, *360*, 3255–3264.
- (38) Wong, T.-W.; Lau, T.-C.; Wong, W.-T. *Inorg. Chem.* **1999**, *38*, 6181–6186.
- (39) Zhang, K.-L.; Xu, Y.; Song, Y.; Zhang, Y.; Wang, Z.; You, X.-Z. *J. Mol. Struct.* **2001**, *570*, 137–143.
- (40) Marvel, C. S.; Aspey, S. A.; Dudley, E. A. *J. Am. Chem. Soc.* **1956**, *78*, 4905–4909.
- (41) Salavati-Niasari, M.; Khansari, A.; Davar, F. *Inorg. Chim. Acta* **2009**, *362*, 4937–4942.
- (42) Durfee, L. D.; Latesky, S. L.; Rothwell, I. P.; Huffman, J. C.; Foltz, K. *Inorg. Chem.* **1985**, *24*, 4569–4573.
- (43) Balsells, J.; Carroll, P. J.; Walsh, P. J. *Inorg. Chem.* **2001**, *40*, 5568–5574.
- (44) Chmura, A. J.; Davidson, M. G.; Jones, M. D.; Lunn, M. D.; Mahon, M. F.; Johnson, A. F.; Khunkamchoo, P.; Roberts, S. L.; Wong, S. S. F. *Macromolecules* **2006**, *39*, 7250–7257.
- (45) Groysman, S.; Sergeeva, E.; Goldberg, I.; Kol, M. *Eur. J. Inorg. Chem.* **2005**, *2005*, 2480–2485.
- (46) Yeori, A.; Groysman, S.; Goldberg, I.; Kol, M. *Inorg. Chem.* **2005**, *44*, 4466–4468.
- (47) Unpublished Results.
- (48) Manna, C. M.; Braitbard, O.; Weiss, E.; Hochman, J.; Tshuva, E. Y. *ChemMedChem* **2012**, in print.
- (49) Ansari, K. I.; Grant, J. D.; Kasiri, S.; Woldemariam, G.; Shrestha, B.; Mandal, S. S. *J. Inorg. Biochem.* **2009**, *103*, 818–826.
- (50) Ansari, K. I.; Grant, J. D.; Woldemariam, G. A.; Kasiri, S.; Mandal, S. S. *Org. Biomol. Chem.* **2009**, *7*, 926–932.
- (51) Ansari, K. I.; Kasiri, S.; Grant, J. D.; Mandal, S. S. *Dalton Trans.* **2009**, 8525–8531.
- (52) Ansari, K. I.; Kasiri, S.; Grant, J. D.; Mandal, S. S. *J. Biomol. Screening.* **2011**, *16*, 26–35.
- (53) Manna, C. M.; Armony, G.; Tshuva, E. Y. *Inorg. Chem.* **2011**, *50*, 10284–10291.
- (54) Meker, S.; Manna, C. M.; Peri, D.; Tshuva, E. Y. *Dalton Trans.* **2011**, *40*, 9802–9809.
- (55) Manna, C. M.; Armony, G.; Tshuva, E. Y. *Chem.—Eur. J.* **2011**, DOI: 10.1002/chem.201102017.
- (56) Manna, C. M.; Tshuva, E. Y. *Dalton Trans.* **2010**, *39*, 1182–1184.
- (57) Chen, H. Y.; Cronin, J. A.; Archer, R. D. *Macromolecules* **1994**, *27*, 2174–2180.
- (58) Chen, H. Y.; Cronin, J. A.; Archer, R. D. *Inorg. Chem.* **1995**, *34*, 2306–2315.
- (59) Woltinger, J.; Backvall, J. E.; Zsigmond, A. *Chem.—Eur. J.* **1999**, *5*, 1460–1467.
- (60) Hille, A.; Gust, R. *Eur. J. Med. Chem.* **2010**, *45*, 5486–5492.
- (61) Lavastre, O.; Illitchev, I.; Jegou, G.; Dixneuf, P. H. *J. Am. Chem. Soc.* **2002**, *124*, 5278–5279.
- (62) Pui, A.; Dobrota, C.; Mahy, J. P. J. *Coord. Chem.* **2007**, *60*, 581–595.